Learning RuBisCO's birth and subsequent environmental adaptation

Ashida, Hiroki

Mizohata, Eiichi

Yokota, Akiho

(Citation)
Biochemical Society Transactions,47(1):179-185

(Issue Date)
2018-12-17

(Resource Type)
journal article

(Version)
Accepted Manuscript

(URL)
https://hdl.handle.net/20.500.14094/90005747

Learning RuBisCO's birth and subsequent environmental adaptation

Hiroki Ashida[1], Eiichi Mizohata[2, 3] and Akiho Yokota[4]

[1]Graduate School of Human Development and Environment, Kobe University, Tsurukabuto, Kobe City 657-8501, Japan

[2]Department of Applied Chemistry, Osaka University, Suita, Osaka 565-0871, Japan

[3]JST-PRESTO, Kawaguchi, Saitama 332-0012, Japan.

[4]Nara Institute of Science and Technology, Ikoma, Nara 630-0192, Japan

Correspondence: AkihoYokota (yokota@bs.naist.jp)

(Abstract)

It is believed that organisms that first appeared after the formation of the earth lived in a very limited environment, making full use of the limited number of genes. From these early organisms' genes, more were created by replication, mutation, recombination, translocation, and transmission of other organisms' DNA; thus, it became possible for ancient organisms to grow in various environments. The photosynthetic CO_2-fixing enzyme RuBisCO began to function in primitive methanogenic archaea and has been evolved as a central CO_2-fixing enzyme in response to the large changes in CO_2 and O_2 concentrations that occurred in the subsequent 4 billion years. In this review, the processes of its adaptation to be

specialized for CO_2 fixation will be presented from the viewpoint of functions and structures of RuBisCO.

Introduction

Billions of years after the earth was formed, the initial microorganisms (believed to be anaerobic archaea) are assumed to have appeared. Among the anaerobic archaea, methanogenic archaea are thought to be responsible for methane production from CO_2, which accounted for almost 100% of the atmosphere, and H_2 produced non-biologically [1]. Recent results suggest that photosynthetic CO_2-fixing enzyme RuBisCO originated from a primitive Calvin-Benson-Bassham (CBB) cycle, the reductive hexulose-phosphate (RHP) pathway, involved in the methane production in *Methanospirillum hungatei* [2] (Figure 1).

In the environmental CO_2 concentration at that time, CO_2 bonding to methanofuran-NH_3^+ (carbamylation), which was the initial reaction of methane production, CO_2 bonding to the activation site Lys201-NH_3^+ of RuBisCO, and the reaction of the substrate CO_2 to C2 of deprotonated ribulose 1,5-bisphosphate (RuBP) at the RuBisCO catalytic site proceeded as chemical reactions [3]. In response to a major environmental change that subsequently declined by 1/2000 of the environmental CO_2 concentration over 4 billion years, methanogenic archaea were restricted to an anaerobic environment containing high concentrations of CO_2 [4]. In contrast, how RuBisCO responded to this change has not been argued sufficiently. In this review, we discuss the mechanism of environmental adaptation of RuBisCO, which has followed the process of sharply decreasing CO_2 concentration and increasing O_2 concentration from almost

zero to 21%.

Questions in RuBisCO *in vivo* activation

Activation mechanism

The reversible activation reaction of RuBisCO proceeds as follows: Lys201-NH_2 (E) binds CO_2 (C) to form Lys201-$NHCOO^-$ (EC), to which Mg^{2+} (M) further coordinated to complete the activated ECM form [5]. The ternary complex is essential for the enzyme to proceed with the deprotonation of C3 of RuBP. The reaction rate of the carbamate formation process among these processes is very slow, but binding of Mg^{2+} to the carbamate progresses very fast [6]. When 44 μM RuBisCO protomer was activated at 112 μM CO_2 at 10 ºC, the activation rate was calculated to be approximately 3 μM/sec and the activated was accomplished in 10 min [7]. Conversely, the rate constant of chemical bonding of CO_2 to the amino group of a model compound monoethanolamine (MEA) is 6.1×10^3/M/sec at 30 ºC [8]. Calculated using this reaction rate constant, the equilibrium in activation should have been reached in 3.2 sec with the RuBisCO protomer and CO_2 concentration used in the biochemical experiment. In contrast, the rate constant of liberation of CO_2 from MEA carbamate is 29.8/sec and its half-life is 0.023 sec, but the half-life at which activated RuBisCO is inactivated under inactivation conditions was 20 sec (Figure 1). The difference in reaction rates between the amino groups and CO_2 cannot be explained completely by the difference in the reaction temperatures used. Below, we discuss how Rubisco was able to accomplish its catalytic function using two molecules of CO_2 independently as a catalysis-supporting molecule and a substrate in the adaptation process of RuBisCO to accomplish a considerable change in the atmospheric gas composition.

Activation by sugar phosphates and NADPH

Ligands of RuBisCO can be classified into three groups, based on their effects on activation [3, 9-11]: (i) positive effectors, e.g., reduced nicotinamide adenine dinucleotide phosphate (NADPH), 6-phosphogluconate (6-PG), inorganic phosphate, and 2-carboxy-D-arabinitol 1,5-bisphosphate enhance activation; (ii) negative effectors, e.g., D-xylulose 1,5-bisphosphate and ribose 5-phosphate facilitate deactivation; and (iii) neutral ligands, e.g., RuBP does not actually promote or inhibit RuBisCO activation [12]. 6-PG and NADPH seems to be especially important as physiological positive effectors. In 6-PG analysed in detail, K_i of 6-PG in competitive inhibition with respect to RuBP was different from K_d determined by the equilibrium binding analysis; K_i was 8.5 μM, but K_d was 37 μM [10]. The promotion of activation of RuBisCO by 6-PG gave a saturation curve and the half-saturation concentration of 6-PG was 50 μM [7]. 6-PG binds to the RuBP-binding site in a competitive manner in the inhibition kinetics, but may adopt a different binding mode in the activation from that inferred in the competitive kinetics. Although NADPH is also a competitive inhibitor of RuBP, there is no difference between K_i and K_m for NADPH during activation; although it is not as much as 6-PG, the binding mode may be different from that of RuBP.

After that, this concept was clarified from the X-ray structural analysis of rice RuBisCO complexed with 6-PG or NADPH [11]. In rice RuBisCO, which was crystallized under the condition including 40 mM 6-PG or NADPH in the presence of CO_2 and 40 mM $MgCl_2$ in the buffer in equilibrium with air, those structures were very different from those expected from the difference between the above K_i, and K_d or K_m. These sugar phosphates were bound to the catalytic site, where the ε-amino group of

Lys-201 was carbamylated and Mg^{2+} was coordinated to the carbamate anion. The position of the carbamyl group oxygen of Lys-201 stabilizing this Mg^{2+} and the position of Asp-203 and Glu-204 carboxyl group oxygen had very similar architecture between 6-PG- and NADPH-bound enzymes. One of the small differences seen in these two enzymes was that the carboxyl groups of 6-PG and the oxygen of the hydroxyl group on C2 were directly coordinated to Mg^{2+} in the former, but in the NADPH enzyme, the adiponyl phosphate oxygen and the C3 hydroxyl group oxygen of the nucleotide ribose stabilized Mg^{2+} via two molecules of water. Conversely, two of the three Mg^{2+}-coordinated water molecules observed in the NADPH complex were substituted by the C1 carboxyl and C2 hydroxyl oxygen atoms of 6-PG. This observation suggests that 6-PG stabilizes the ECM form by directly interacting with Mg^{2+}, unlike the indirect and relaxed interaction between RuBisCO and NADPH. These structural differences may explain the observed differences in stabilizing the activated form of RuBisCO.

It is interesting to analyse the functions of 6-PG and NADPH from kinetic data of the activities of enzymes [7]. When RuBisCO, which had been activated (ECM), was diluted with a system without CO_2 or a buffer containing EDTA, RuBisCO was inactivated with a half-life of about 20 sec. The addition of 6-PG or NADPH to this RuBisCO inactivation reaction caused the half-life to increase to 1,800 and 300 sec, respectively. In other words, the ECM form of Rubisco which kept its activated state with 6-PG or NADPH maintained the active state for a long time even in the presence of EDTA (Fig. 3). The slight difference seen in 6-PG and NADPH seems to be due to only a slight difference in structure taken by RuBisCO when bound to the effectors.

Activation and activase

That the ECM form constitutes a complex with carboxyl groups from Glu-203 and Asp-204 around Lys-201 in order for RuBisCO to exhibit a CO_2 fixation reaction has been proven to be essential through many pioneering RuBisCO discoveries over the half-century since the discovery of the enzyme [5]. RuBisCO activase is deeply involved in this process [13, 14]. RuBisCO activase dose not catalyze directly the activation of RuBisCO, but removes various sugar phosphate inhibitors such as RuBP bound to inactive RuBisCO and gives a chance to catalytic sites of RuBisCO to be activated. A group from the Max Plank Research Institute has proposed an intriguing challenge to this process via analysis of the structure of RuBisCO activase in the last several years [15, 16], suggesting that RuBisCO activase from tobacco functions as a hexamer .

It has been known for some time that the concentration of RuBisCO activase in chloroplasts is rather low. When exerting its function on RuBisCO, if the activase exhibits its functions by constituting a hexamer in vivo as proposed by Hayer-Hartl's group; so RuBisCO holoenzyme (L_8S_8) in the chloroplast is 3 μmol/m^2 and the activase (A_6, hexamer of activase) has been estimated to be 0.57 μmol/m^2 [17]. In the measurements by Mate et al. [18], these values were 2.5 and 0.16 μmol/m^2, respectively. In these activase antisense experiments, where the activase content was further reduced to one-fifth of the wild-type level, the gas exchange rate was not affected; so, the amount of activase required by 1 μmol/m^2 of RuBisCO holoenzyme is 0.03 to 0.11 μmol/m^2 for photosynthesis to proceed without any retardation. These results suggested that relatively low concentration of activase is enough for RuBisCO activation.

How does RuBisCO keep its activated state?

As pointed out above, the carbamate formation of the ε-amino group of Lys-201 for RuBisCO activation required a duration 180-times longer than the chemical carbamylation of MEA. This may be because carbamylation of Lys-201 not only proceeds as a chemical reaction, but also involves a structural change in the RuBisCO protein, which takes longer time. For that reason, the ECM form of RuBisCO protects Mg^{2+} from being chelated by EDTA (Figure 2).

Such slow activation/deactivation actually measured by RuBisCO is convincing if we consider that these processes involve the structural change of the RuBisCO protein. In fact, Vater et al. [19] revealed structural changes of RuBisCO during activation by CO_2 and $Mg^{2+}$with *p*-toluidinonapthalene-6-sulfonate (TNS), a hydrophobic fluorescent reporter. Detailed analysis of RuBisCO activation/inactivation by Lorimer and his colleagues [6, 7] clarified that the half-life of inactivation was further increased when RuBisCO activated in the presence of 6-PG and NADPH was inactivated by adding EDTA; half-lives were 78,000 and 13,000 times, respectively, longer than the case of CO_2 release from carbamylated MEA. When RuBisCO activated by these effectors was placed in a reaction system containing saturated concentrations of RuBP and CO_2, the enzyme showed full activity without delay [7]. This indicates that these effectors are promptly released from the catalytic sites but cause RuBisCO to keep its activated conformation for a long period in the absence of the effectors, where the substrate RuBP may be involved in maintaining the activated state during the carboxylation reaction [11, 13].

The minimum amount of RuBisCO activase hexamer required for 1 μmol/m^2 of RuBisCO holoenzyme is 0.03 to 0.11 μmol/m^2, as discussed above. Activase is needed in removal of various sugar phosphate inhibitors such as RuBP bound to inactive

RuBisCO and structural analogues of RuBP formed during catalysis. It seems that once activase exerts its function, RuBisCO may adopt a conformation of the activated ECM form with aid of positive effectors [11].

How did RuBisCO develop the capacity to use low concentrations of CO_2 preferentially over great concentrations of O_2 in the present atmosphere?

The CO_2/O_2 specificity factor of RuBisCO, S_{rel}, determines the relative rates of the carboxylase reaction to oxygenase reaction at any given CO_2 and O_2 concentrations. S_{rel} has a special meaning in kinetic parameters of RuBisCO and is calculated by the equation, $(k_{cat}^{c}/K_m^{c})/(k_{cat}^{o}/K_m^{o})$, where k_{cat}^{c}, k_{cat}^{o} and K_m^{c}, K_m^{o} are the maximum catalytic turnover rates and Michaelis constants for CO_2 and O_2, respectively [20]. RuBisCO with high S_{rel} values have lower reactivity for O_2, and are specialized in catalysis of the carboxylase reaction. S_{rel} values are 70–94 among plant species, 54–83 among green algal RuBisCOs, 38–56 from cyanobacterial RuBisCOs, and 26–53 among bacterial RuBisCOs. On the other hand, in red-like RuBisCOs, S_{rel} is 40–75 for RuBisCOs from phototrophic bacteria and 105-238 for RuBisCOs from non-green algae, such as red algae and diatoms.

It has become clear that the extensive diversity of RuBisCO's S_{rel} was attained in the process of evolution of this enzyme. The problem remained to be discussed in this review is how RuBisCO was able to produce a difference of 500 times in S_{rel} [3]. Here may be the point of functional improvement of this important enzyme in the future. In the reaction of RuBisCO, it does not happen that this enzyme recognizes the gaseous substrate molecule specifically and forms an enzyme substrate complex, unlike usual enzymes. It is hypothesized that the reason why

plant and red algal RuBisCOs catalyze the carboxylase reaction more preferentially as compared with the oxygenase reaction in the process of evolution is that their active sites have a higher affinity for the transition state for carboxylation than that for oxygenation [21]. A structural resemblance between transition state for CO_2 addition and carboxylated product, 2-carboxy-3-ketoarabinitol 1,5-bisphosphate should enable the higher S_{rel}. On the other hand, such strategy causes a tight binding of the intermediate, leading to a decreased maximum carboxylation rate. This is in agreement with the propensity of the inverse correlation between S_{rel} and maximum carboxylation rate.

A structural feature involved in S_{rel} has recently been proposed. Lun et al. investigated the migration of CO_2 and O_2 in and around RuBisCO using molecular dynamics simulations [22]. Although they cannot detect any cavities providing a route for gaseous substrates to the active site, interestingly, surface of hexadecameric RuBisCO binds CO_2 stronger than it does O_2. Importantly, the simulations showed a preference of CO_2 for amino acids with small hydrophobic side chains, such as alanine, valine, leucine, and isoleucine, and for the sulfur-containing cysteine residue (Note that these are neutral amino acids). These results suggested that CO_2 is guided toward the reaction center through a CO_2 binding region during the active site opening. However, the study did not analyze to compare RuBisCOs from different species with different S_{rel} values. This gave us the idea that the content of neutral residue around active site of RuBisCO might be correlate with S_{rel}. Figure 3 shows the electrostatic potentials on the solvent accessible surface of closed forms of RuBisCOs from verious sources. The top and side views for overall structures show a diversity in distribution of the positive, negative and neutral regions. We cannot

find any relationship between S_{rel} and distribution of these regions in overall structures. The negative potential dominates the entrance of the catalytic site of RuBisCO. The entrance is composed of *N*-terminal tail, residues 46–49, catalytic loop 6, and *C*-terminal tail. In particular, between RuBisCOs from *Synechococcus* sp. PCC6301 and *Chlamydomonas reinhardtii*, the amino acid residues constituting the entrance are conserved and show a remarkable negative potential. The negative potential is derived from acidic side chains and main chain oxygens of the residues. Compared with those RuBisCOs, RuBisCO from *Oryza sativa* with higher S_{rel} gains a neutral potential at the entrance by a E464A substitution. Similary, RuBisCO from *Galdieria partita* earns even higher neutrality than RuBisCO from *O. sativa* by D19P and E468N substitutions. It is interesting to see a correlation that S_{rel} improves as the neutrality of the entrance increases. At the present time, it is unclear whether the neutrality of the entrance is involved in determination of S_{rel}, but this may be an interesting target to analyze. The S_{rel} of Rubisco mutants with increased neutrality around the catalytic pocket may be improved. Considering that hydrophobic region prefers CO_2 rather than O_2, the hydrophobicity of the active site entrance may contribute to increase S_{rel} [23]. Similarly, also in the partial reaction of phosphoenolpyruvate carboxylase (PEPC) which catalyses the fixing reaction of CO_2 derived from HCO_3^- in phosphoenolpyruvate (PEP) to C1 proceeds in the neutral pocket of the reaction centre [24], implying that the charge-neutral environment may play an important role for carboxylase reaction in both RuBisCO and PEPC.

The neutral environment may affect gaseous substrates at the entrance to the catalytic pocket. Here is an interesting example. Many wetland species of plants form aerenchyma and a barrier to radial O_2 loss in roots to enhance internal O_2 diffusion to

the root apex [25]. O_2 diffusion is suppressed by covering this transit tissue with charge-nutral suberin. Considering that such neutral regions repel O_2, local concentration of CO_2 relative to O_2 in charge-neutral entrance of RuBisCO active site may increase by exclusion of O_2. If RuBisCO gradually changed the reaction centre to raise the S_{rel} in response to billions of years of a drastic change in the global environment, it is worth considering the idea that the entrance gate of gaseous substrates of RuBisCO was changed gradually to neutral to increase the CO_2/O_2 ratio in the reaction centre space.

Abbreviations:

EDTA, ethylenediaminetetraacetate; MEA, monoethanolamine; NADPH, reduced nicotinamide adenine dinucleotide phosphate; PEP, phosphoenolpyruvate; PEPC, phosphoenolpyruvate carboxylase; 6-PG, 6-phosphogluconate; RHP, reductive hexulose phosphate; RuBP, ribulose 1,5-bisphosphate; RuBisCO, ribulose 1,5-bisphosphate carboxylase/oxygenase; S_{rel}, CO_2/O_2 specificity factor; TNS, *p*-toluidinonapthalene-6-sulfonate.

Author contribution

A.Y. was invited from the Publisher to contribute a review and made the structure of the article with H.A. E.M. analyzed protein structures and electrostatic potentials on the solvent accessible surface of RuBisCO. A.Y., H.A. and E.M. contributed equally in preparing the manuscript.

Funding

RuBisCO researches were funded by the Ministry of Education, Culture, Sports, Science and Technology and the Ministry of Economy, Trade and Industry. H.A. is also partly supported by JSPS KAKENHI Grant Number 17H03964, and E.M. is partly supported by JST, PRESTO Grant Number JPMJPR17GB.

Competing Interests

The authors declare that there are no competing interests associated with the manuscript.

References

1 Huang, R., Sun, W., Liu, J., Ding, X., Shaobang Peng, S. and Zhan, W. (2016) The H_2/CH_4 ratio during serpentinization cannot reliably identify biological signatures. Sci. Rep. 6:33821. http://doi.org/10.1038/srep33821.

2 Kono, T., Mehrotra, S., Endo, C., Kizu, N., Matusda, M., Kimura, H. et al. (2017) A RuBisCO-mediated carbon metabolic pathway in methanogenic archaea. *Nat. Commun.* **8**:14007. http://doi.org/10.1038/ncomms14007

3 Yokota, A. (2017): Revisiting RuBisCO, *Biosci. Biotechnol. Biochem.* **81**, 2039-2049. http://doi.org/10.1080/09168451.2017.1379350

4 Thauer, R. K., Kaster, A. K., Seedorf, H., Buckel, W. and Hedderich, R. (2008) Methanogenic archaea: ecologically relevant differences in energy conservation. *Nat. Rev. Microbiol.* **6**:579-591. http://doi.org/10.1038/nrmicro1931.

5 Cleland, W. W., Andrews, T. J., Gutteridge, S., Hartman, F. C. and Lorimer, G. H. (1998) Mechanism of Rubisco: The carbamate as general base. *Chem. Rev.* **98** 549-562. http://doi.org/10.1021/cr970010r.

6 Lorimer, G. H., Badger, M. R. and Andrews, T. J. (1976) The activation of ribulose-1,5-bisphosphate carboxylase by carbon dioxide and magnesium ions. Equilibria, kinetics, a suggested mechanism, and physiological implications. *Biochemistry* **15**, 529-536. http://doi.org/10.1021/bi00648a012.

7 Badger, M. R. and Lorimer, G. H. (1981) Interaction of sugar phosphates with the catalytic site of ribulose-1,5-bisphosphate carboxylase. *Biochemistry* **20**, 2219-2225. http://doi.org/10.1021/bi00511a023.

8 McCann N, Phan D, Wang X, Conway, W., Burns, R., Attalla, M., Puxty, C. and Maeder, M.

(2009) Kinetics and mechanism of carbamate formation from CO_2 (aq), carbonate species, and monoethanolamine in aqueous solution. *J. Phys. Chem. A.* **113**, 5022–5029 http://doi.org/10.1021/jp810564z

9 McCurry SD, Pierce J, Tolbert NE, et al. On the mechanism of effector-mediated activation of ribulose bisphosphate carboxylase/oxygenase. *J. Biol. Chem.* 1981 Jul 10;256(13):6623-6628.

10 Douglas B. Jordan, Raymond Chollet,* and William L. Ogren (1983) Binding of phosphorylated effectors by active and inactive forms of ribulose 1,5-bisphosphate carboxylase. *Biochemistry* **22**, 3410–3418 http://doi.org/10.1021/bi00283a017

11 Matsumura, H., Mizohata, E., Ishida, H., Kogami, A., Ueno, T., Makino, A.et al. (2012) Crystal structure of rice Rubisco and implications for activation induced by positive effectors NADPH and 6-phosphogluconate. *J. Mol. Biol*. **422**, 75-86 http://doi.org/10.1016/j.jmb.2012.05.014

12 Zhu, G, and Jensen R. G. (1991) Fallover of ribulose 1,5-bisphosphate carboxylase/oxygenase activity. Decarbamylation of catalytic sites depends on PH. *Plant Physiol.* **97,** 1354-1358.

13 Somerville, C. R., Portis, A. R. and Ogren, W. L. (1982) A mutant of *Arabidopsis thaliana* which lacks activation of RuBP carboxylase *in vivo. Plant Physiol*. **70**, 381-387. https://doi.org/10.1104/pp.70.2.381

14 Portis, A. R., Jr., Li, C., Wang, D. (2008) Salvucci ME, Regulation of Rubisco activase and its interaction with Rubisco. *J Exp Bot*. **59**, 1597-1604.http://doi.org/ 10.1093/jxb/erm240.

15 Stotz, M., Mueller-Cajar, O., Ciniawsky, S., Wendler, P., Hartl, F. U., Bracher, A. , Hayer-Hartl, M. (2011) Structure of green-type Rubisco activase from tobacco. *Nat. Struct. Mol. Biol.***18**, 1366-1370 http://doi.org/ 10.2210/pdb3T15/pdb

16 Mueller-Cajar, O., Stotz, M., Wendler P, Hartl, F. U., Bracher, A . and Hayer-Hartl, M. (2011) Structure and function of the AAA+ protein CbbX, a red-type Rubisco activase. *Nature* **479**, 194-199 http://doi.org/10.1038/nature10568

17 Eckardt, N.,A., Snyder, G. W., Portis, A. R., Jr. and Orgen, W. L. (1997) Growth and photosynthesis under high and low irradiance of Arabidopsis thaliana antisense mutants with reduced ribulose-1,5-bisphosphate carboxylase/oxygenase activase content. *Plant Physiol*. **113**, 575-586 http://doi.org/10.1104/pp.113.2.575

18 Mate, C. J., von Caemmerer, S., Evans, J. R. Hudson, G. S. and Andrews, T. J. (1996) The relationship between CO_2-assimilation rate, Rubisco carbamylation and Rubisco activase content in activase-deficient transgenic tobacco suggests a simple model of activase action. *Planta* **198**, 604-613 http://doi.org/ 10.1007/BF00262648

19 Vater, S., Salnikow, J. and Kleinkauf, H. (1977) *Biochem. Biophys. Res. Commun.* **74**, 1618-1625 https://doi.org/10.1016/0006-291X(78)91506-1.

20. Ashida H, Yokota A, Increasing photosynthesis/RuBisCO and CO_2-concentrating mechanisms.

In: Murray M-Y editor. Comprehensive biotechnology, second edition, Vol 4. Elsevier. 2011, p. 165–176 ISBN:978-0-08-088504-9

21 Tcherkez G. G. B., Farquhar, G. D. and Andrews, T. J. (2006) Despite slow catalysis and confused substrate specificity, all ribulose bisphosphate carboxylases may be nearly perfectly optimized. *Proc. Nat. Acad. Sci. USA* **103**, 7246-7251 https://doi.org/10.1073/pnas.0600605103

22 van Lun, M., Hub, J. S., van der Spoel, D. and Andersson, I. (2014) CO_2 and O_2 distribution in rubisco suggests the small subunit functions as a CO_2 reservoir. *J. Am. Chem. Soc.* **136**, 3165−3171 http://doi.org/10.1021/ja411579b

23 Endeward, V., Al-Samir, S., Itel, F. and Gros, G. (2014) How does carbon dioxide permeate cell membranes? A discussion of concepts, results and methods. *Front. Physiol.* **4**, 382 http://doi.org/10.3389/fphys.2013.00382

24 Izui, K., Matsumura, H., Furumoto,T. and Kai, Y. (2004) Phospho*enol*pyruvate carboxylase: A New era of structural biology. *Annu. Rev. Plant Biol.* **55**, 69–84 http://doi.org/ 10.1146/annurev.arplant.55.031903.141619

25 Shiono, K., Ogawa, S., Yamazaki, S., Hiroko Isoda, H., Fujimura, T., Nakazono, M., et al. (2011) Contrasting dynamics of radial O_2-loss barrier induction and aerenchyma formation in rice roots of two lengths. *Ann. Bot.* **107**, 89–99 http://doi.org/ doi:10.1093/aob/mcq221

Figure legends

Figure 1. Proposed primitive Calvin-Benson-Bassham cycle (reductive hexulose-phosphate (RHP) pathway) and related metabolic processes in archaea.

The RHP pathway (highlighted in yellow) has metabolic links to methanogenesis via methylene-H_4MPT, which may be synthesized with formaldehyde released from the RHP pathway. The successive black arrows show multiple reaction steps. The RHP pathway (red lines and arrows) is superimposed on the CBB cycle (green lines and arrows), and reaction steps from Ru5P to F6P are common in both cycles. Missing CBB cycle steps in *Methanospillirum hungatei* are indicated by grey dashed lines and arrows. Ru5P, ribulose 5-phosphate; RuBP, ribulose 1,5-bisphosphate; 3-PGA, 3-phosphoglycerate; BPG, 1,3-diphosphoglycerate; GAP, glyceraldehyde 3-phosphate; DHAP, dihydroxyacetone phosphate; FBP, fructose 1,6-bisphosphate; F6P, fructose

6-phosphate; Hu6P, D-arabino-3-hexulose 6-phosphate; FA, formaldehyde; E4P, erythrose 4-phosphate; Xu5P, xylulose 5-phosphate; SBP, sedoheptulose 1,7-bisphosphate; S7P, sedoheptulose 7-phosphate; R5P, ribose 5-phosphate; H_4MPT, tetrahydromethanopterin; MFR, methanofuran; PRK, phosphoribulokinase; PGK, 3-phosphoglycerate kinase; GAPDH, glyceraldehyde 3-phosphate dehydrogenase; TPI, triose phosphate isomerase; FBPase, fructose 1,6-bisphosphatase; TK, transketolase; SBPase, sedoheptulose 1,7-bisphosphatase; RPE, ribulose 5-phosphate 3-epimerase; RPI, ribose 5-phosphate isomerase; PHI, 6-phospho-3-hexulose 6-phosphate; HPS, D-arabino-3-hexulose 6-phosphate synthase.

Figure 2. Effector-dependent suppression of the deactivation of RuBisCO.

This figure is a recasting of Fig. 4 of reference 7 and includes additional calculations as explained in the text. The enzyme (approximately 7 mg/mL) was first activated in Bicine buffer (pH 8.2) containing 20 mM $MgCl_2$ and 5 mM $NaHCO_3$. At time zero, 5 µL (35 µg of enzyme) of the solution was added to 400 µL of Bicine buffer (pH 7.8) containing 1 mM EDTA and 0.6 mM $NaH^{14}CO_3$ at 10 °C (light blue line). Where appropriate, this mixture contained 0.1 mM 6-PG (black line) or 0.2 mM NADPH (green line). At the indicated times, 10 µl of 20 mM RuBP was introduced to measure the remaining activity at that time for 30 sec. A_t is the activity at time t, and A_i is the initial activity. *Inset*: This panel replotted the reaction courses of lines 1 and 3 for the initial 20 sec. Red line is the course of the chemical reaction of CO_2 released from MEA carbamate as calculated by the following equation: $A_t/A_i = e^{-kt}$, where k is the rate constant of the liberation of CO_2 from MAE carbamate and where t is the time in sec. A_t is the concentration of MEA carbamate remaining at time t, and A_i is the initial concentration.

Figure 3. Crystal structures and surface properties of hexadecameric RuBisCOs from a cyanobacterium *Synechococcus* sp. PCC6301 (PDB code: 1RBL), a green alga *Chlamydomonas reinhardtii* (1IR2), a higher plant *Oryza sativa* (1WDD) and a red alga *Galdieria partita* (1BWV). Protein structures and electrostatic potentials on the solvent accessible surface were drawn with PyMOL/APBS (www.pymol.org). Upper and middle figures show top and side views of overall structures, and lower figures display the magnified view around the entrance of the catalytic site. In the left figure (A), *N*-terminal tail (residues 9–22), residues 46-49, loop 6 (331–338), *C*-terminal tail (460–475) and the remaining part of a L2 dimer unit are coloured cyan, green magenta, yellow and light grey, respectively, and the other subunits are dark grey. In the right figures (B), the positive, negative and neutral surfaces are shown in blue, red and white, respectively.

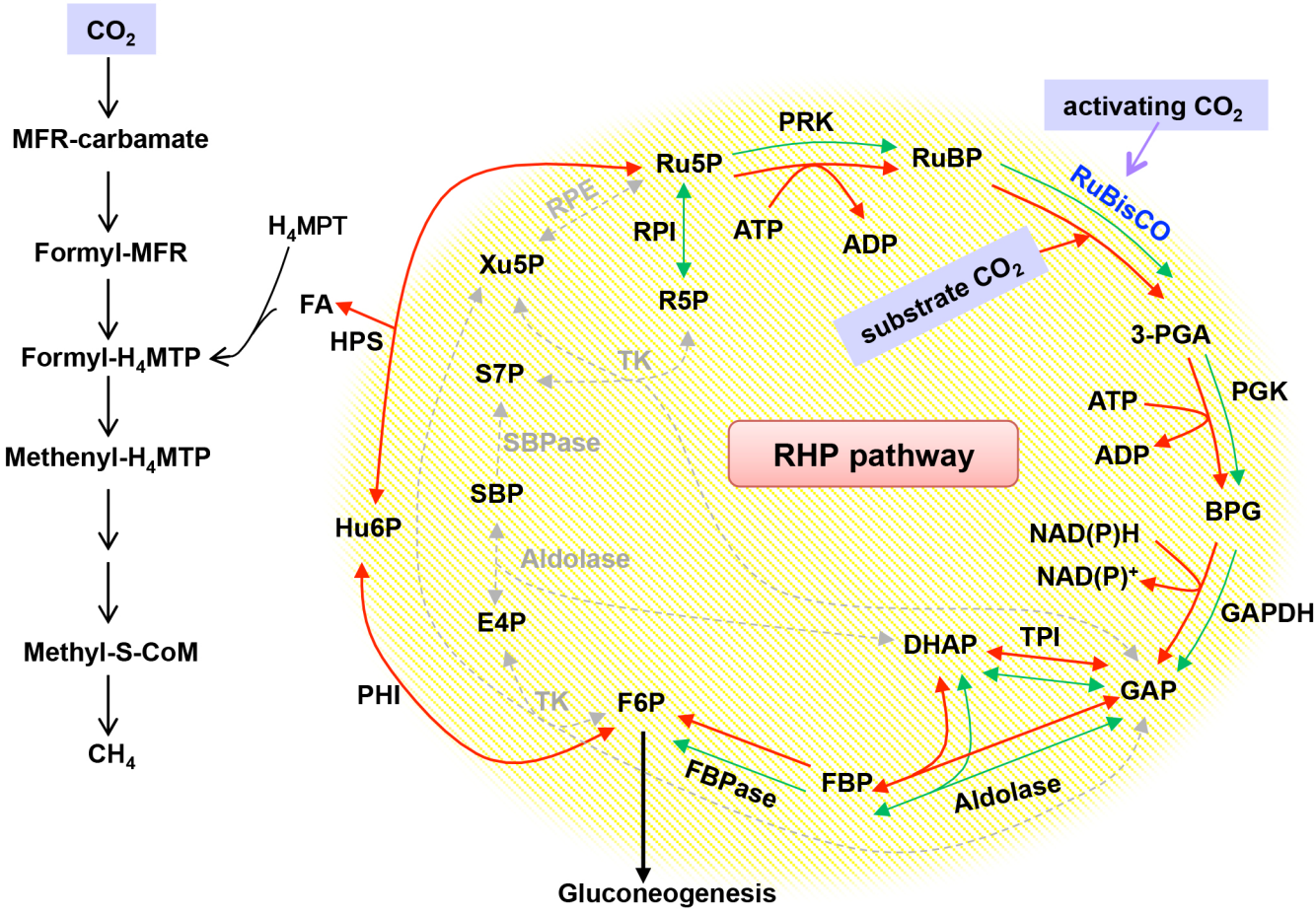
CO2
MFR-carbamate
Formyl-MFR
Formyl-H4MTP
Methenyl-H4MTP
Methyl-S-CoM
CH4
H4MPT
FA
HPS
Hu6P
PHI
F6P
Gluconeogenesis
FBPase
FBP
Aldolase
TK
E4P
SBP
SBPase
S7P
TK
Xu5P
RPE
Ru5P
RPI
R5P
PRK
ATP
ADP
RuBP
activating CO2
RuBisCO
substrate CO2
3-PGA
ATP
ADP
PGK
BPG
NAD(P)H
NAD(P)+
GAPDH
DHAP
TPI
GAP
RHP pathway

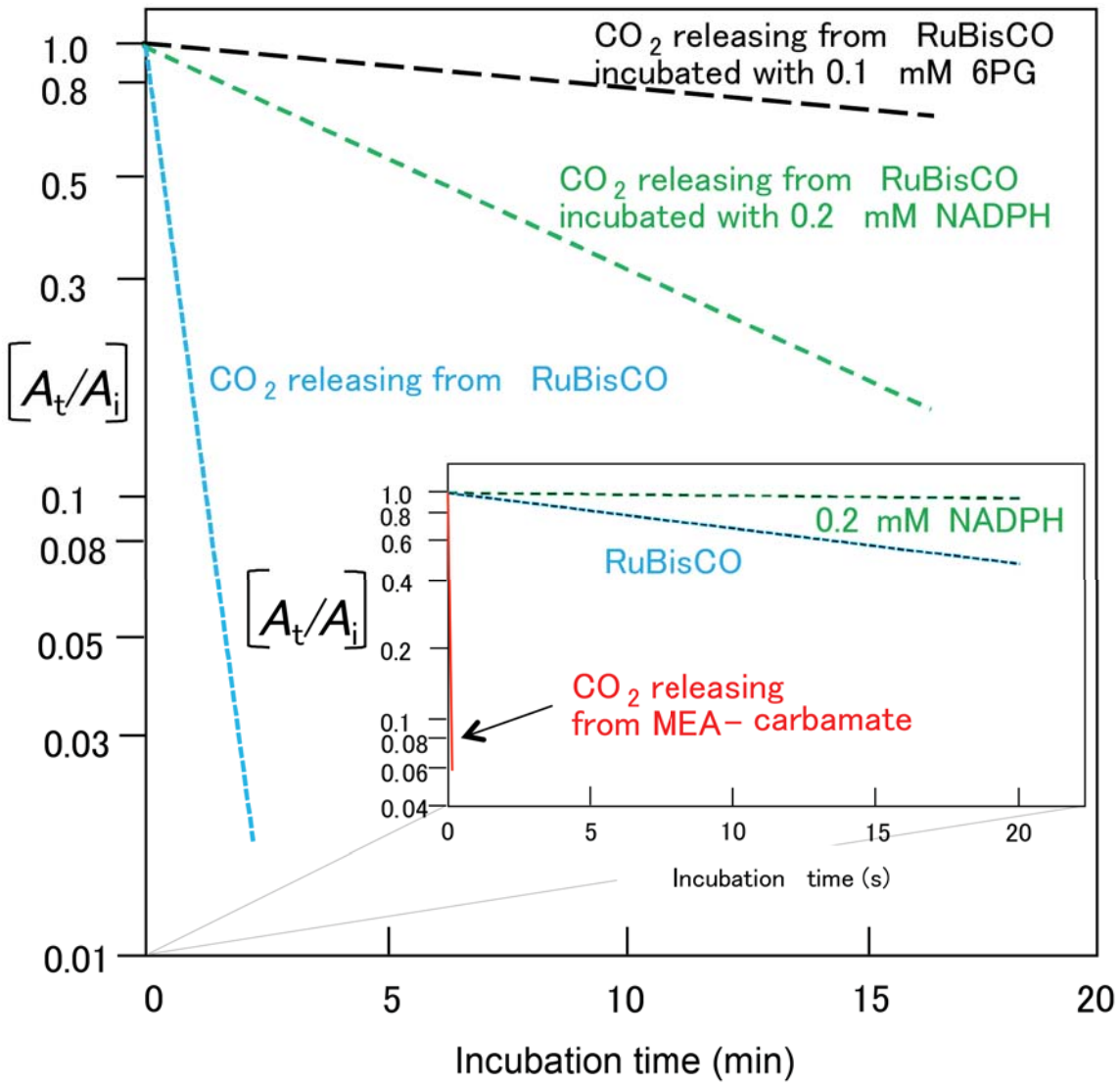
CO 2 releasing from RuBisCO incubated with 0.1 mM 6PG
CO 2 releasing from RuBisCO incubated with 0.2 mM NADPH
CO 2 releasing from RuBisCO
[At/Ai]
1.0
0.8
0.5
0.3
0.1
0.08
0.05
0.03
0.01
0
5
10
15
20
Incubation time (min)
0.2 mM NADPH
RuBisCO
CO 2 releasing from MEA– carbamate
0.6
0.4
0.2
0.06
0.04
Incubation time (s)

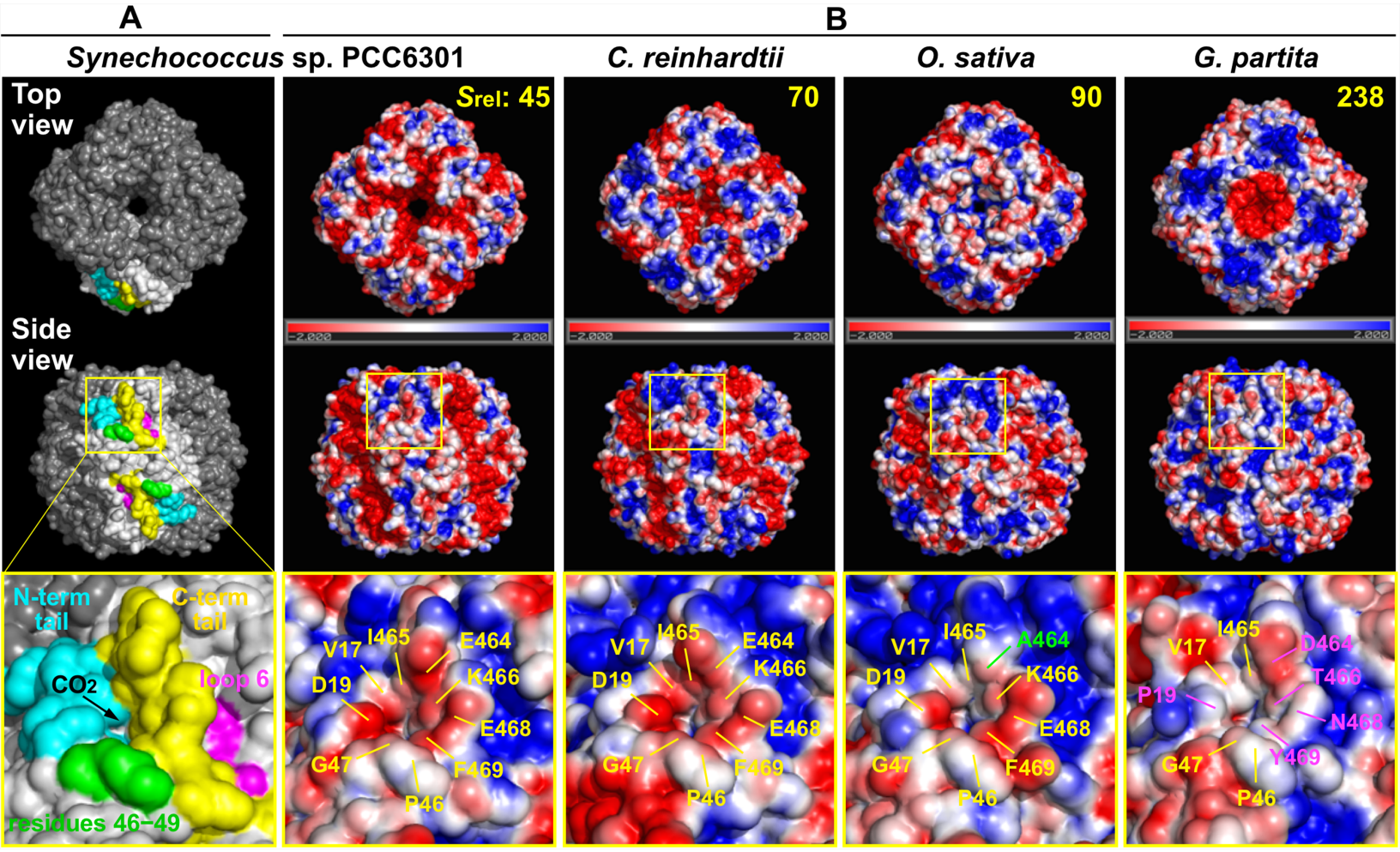
A
B
Synechococcus sp. PCC6301
C. reinhardtii
O. sativa
G. partita
Top view
Side view
Srel: 45
70
90
238
−2.000
2.000
N-term tail
C-term tail
CO2
loop 6
residues 46–49
V17
I465
E464
D19
K466
E468
G47
F469
P46
A464
P19
D464
T466
N468
Y469